Author Manuscript

Author Manuscript

Author Manuscript

Author Manuscript

HHS Public Access

Author manuscript

Sci Immunol. Author manuscript; available in PMC 2024 April 10.

Published in final edited form as:

Sci Immunol. 2024 March 15; 9(93): eadh5318. doi:10.1126/sciimmunol.adh5318.

RORγt upregulates RAG gene expression in DP thymocytes to expand the *Tcra* repertoire

Abani Kanta Naik[1], **Danielle J. Dauphars**[1], **Elizabeth Corbett**[2], **Lunden Simpson**[1], **David G. Schatz**[2], **Michael S. Krangel**[1]

[1]Department of Integrative Immunobiology, Duke University School of Medicine; Durham NC, USA

[2]Department of Immunobiology and Department of Molecular Biophysics and Biochemistry, Yale University School of Medicine; New Haven CT, USA

Abstract

RAG gene expression increases as thymocytes transition from the $CD4^{-}CD8^{-}$ double negative (DN) to the $CD4^{+}CD8^{+}$ double positive (DP) stage, but the physiological importance and mechanism of transcriptional upregulation are unknown. Here we show that a DP-specific component of the RAG anti-silencer (DPASE) provokes elevated RAG gene expression in DP thymocytes. Mouse DP thymocytes lacking the DPASE display RAG gene expression equivalent to that in DN thymocytes, but this supports only a partial *Tcra* repertoire due to inefficient secondary Vα-Jα rearrangement. These data indicate that RAG gene upregulation is required for a replete *Tcra* repertoire, and that RAG expression is fine-tuned during lymphocyte development to meet the requirements of distinct antigen receptor loci. We further show that transcription factor RORγt directs RAG upregulation in DP thymocytes by binding to the DPASE, and that RORγt influences the *Tcra* repertoire by binding to the *Tcra* enhancer. These data, plus prior work showing RORγt to control *Tcra* rearrangement by regulating DP thymocyte proliferation and survival, reveal RORγt to orchestrate multiple pathways that support formation of the *Tcra* repertoire.

One sentence summary:

RORγt directs elevated RAG gene expression in DP thymocytes that is essential to generate a replete *Tcra* repertoire.

Author contributions: A.K.N., D.G.S., and M.S.K. conceived and designed the experiments. A.K.N., E.C., and L.S. performed the experiments (E.C. performed immunoblots; L.S. created the ΔRORE VL3-3M2 mutant and assayed RAG gene expression; A.K.N. performed all other experiments). A.K.N., D.J.D., E.C., D.G.S., and M.S.K. analyzed the experiments. A.K.N. and M.S.K. wrote the manuscript.

Competing interests: The authors declare no competing financial interests.

Data and materials availability: TCRα repertoire sequencing is deposited in the Gene Expression Omnibus (GSE225627). All other data needed to evaluate the conclusions of the paper are present in the paper or the Supplementary Materials, including raw data used to generate figures (see Data file S1). Mice are available under a materials transfer agreement (MTA).

Author Manuscript Author Manuscript Author Manuscript Author Manuscript

Introduction

The vertebrate adaptive immune system can recognize and respond to a broad array of pathogens by virtue of highly diverse antigen receptor repertoires expressed by T and B lymphocytes. These repertoires are assembled in developing lymphocytes by V(D)J recombination, a site-specific DNA recombination process that depends on the products of recombination activating genes 1 and 2 (*Rag1* and *Rag2*). RAG1 and RAG2 (collectively, RAG) proteins form a hetero-tetrameric nuclease that binds to recombination signal sequences flanking T cell receptor (TCR) and immunoglobulin variable (V), diversity (D), and joining (J) gene segments, and then cleaves between the recombination signal sequences and coding gene segments to initiate V(D)J recombination (1). RAG proteins also bind thousands of sites outside of antigen receptor loci, thereby posing a threat to lymphocyte genome integrity (2). Thus, B and T lymphocytes have evolved stringent mechanisms to express *Rag1* and *Rag2* only during specific windows of lymphocyte development when antigen receptor loci are poised to undergo V(D)J recombination (3).

In the T cell lineage, RAG expression first occurs in $CD4^{-}CD8^{-}$ double negative (DN) thymocytes to mediate recombination of the *Tcrb*, *Tcrg* and *Tcrd* genes (3). The RAG genes are transiently suppressed following productive *Tcrb* recombination in developing αβ lymphocytes and are then re-expressed as thymocytes transition to the $CD4^{+}CD8^{+}$ double positive (DP) stage to mediate *Tcra* recombination. Following productive *Tcra* recombination and αβ TCR-mediated signaling for positive selection, RAG expression is extinguished in late-stage thymocytes and peripheral T lymphocytes. Such silencing also occurs in developing γδ T lymphocytes following productive *Tcrg* and *Tcrd* recombination in DN thymocytes. Similar to αβ T lymphocyte development, B cell development is characterized by two distinct waves of RAG gene expression, the first to mediate *Igh* rearrangement, and the second to mediate *Igk* and *Igl* rearrangement (3). Dysregulation of RAG gene expression has pathological consequences in mouse models (4, 5).

Rag1 and *Rag2* are tightly linked in a tail-to-tail configuration on mouse chromosome 2. Although T and B lymphocytes display similar biphasic RAG gene expression programs, these programs are directed by distinct, lineage-specific *cis*-regulatory elements (3, 6). Thymic regulation of the RAG locus is orchestrated by an enhancer called the anti-silencer element (ASE) (7, 8) or the RAG-T cell enhancer (R-TEn) (9), located 73kb upstream of *Rag2*. ASE-deleted mice display substantial reductions in *Rag1* and *Rag2* gene expression in DN and DP thymocytes and developmental blocks at both stages but display no perturbations in B cell development (7, 9). These activities were mapped to a small portion of the ASE region called R-TEn peak1 (9), which includes the previously defined core ASE enhancer (8). For simplicity, we will henceforth refer to this regulatory element as the “core ASE”. The ASE regulates *Rag1* and *Rag2* promoter activity by creating an interaction hub that involves all three elements; this is dependent on the binding of transcription factors E2A, Gata3, and Runx1 to the core ASE (8–10). Hub formation and RAG gene expression also depend on Special AT-rich binding protein 1 (SATB1), which binds to multiple sites across the RAG locus (8).

Author Manuscript Author Manuscript Author Manuscript Author Manuscript

A striking feature of thymocyte development is that RAG gene expression is several-fold higher in DP thymocytes than in DN thymocytes (11). The significance of elevated RAG expression in DP thymocytes is not fully understood because lower expression in DN thymocytes is already sufficient to support the rearrangement of multiple TCR loci (*Tcrb*, *Tcrg*, and *Tcrd*). The mechanism of upregulation is also poorly understood, since most transcription factors critical for thymocyte expression of RAG genes, including E2A, Gata3, Runx1, and Ikaros, occupy the ASE as early as the DN stage (9), and they do not have expression patterns that might explain upregulated expression in DP thymocytes. SATB1 supports RAG expression and is upregulated in DP thymocytes (8), but the breadth of its binding and its effects on the DP thymocyte transcriptional program make it difficult to discriminate direct from indirect effects on gene expression (12, 13). Thus, neither the mechanism nor the physiological importance of DP-specific elevation of RAG expression is currently understood.

In this study, we have identified and characterized a distinct, DP-specific, open chromatin region in the RAG locus that flanks the core ASE (hereafter, DPASE). Analysis of DPASE-deleted mice and a DPASE-deleted cell line revealed that this regulatory region is necessary for RAG upregulation in DP compared with DN thymocytes. RAG expression in DP thymocytes without upregulation resulted in disruption of *Tcra* repertoire formation due to delayed kinetics of secondary *Tcra* recombination. Further characterization revealed that RORγt binds to the DPASE and is essential for DPASE-mediated RAG upregulation. We report that RORγt also facilitates secondary *Tcra* rearrangements by direct binding to the *Tcra* enhancer (Eα). These observations, coupled with prior studies demonstrating that RORγt regulates secondary *Tcra* rearrangement by supporting DP thymocyte proliferation and survival (14, 15), reveal RORγt to be a multi-faceted regulator of the *Tcra* repertoire.

Results

The RAG ASE region contains an element that displays DP-specific chromatin accessibility

To identify *cis*-regulatory elements that might account for developmental stage-specific upregulation of RAG genes in DP thymocytes, we analyzed a recently published assay for transposase-accessible chromatin using sequencing (ATAC-seq) dataset comparing DN, DP, CD4 single positive (CD4SP), and CD8 single positive (CD8SP) thymocytes (16). We identified several regions whose accessibility increased in DP thymocytes and was then extinguished in CD4SP and CD8SP thymocytes (Fig. S1A). Two such sites were the *Rag1 and Rag2* promoters, likely a reflection of their transcriptional activities (Fig. S1B). A third site was in the ASE region. One open chromatin peak in the ASE region corresponds to the previously studied core ASE (8–10) (Fig. 1A and fig. S1A). This site was highly and equally accessible in DN and DP thymocytes but inaccessible in CD4SP and CD8SP thymocytes. However, a second site, immediately adjacent to the core ASE, displayed a DP-specific pattern of accessibility. We refer to this as the DPASE (R-TEn peak 2 according to Miyazaki (9)). An additional DP-specific peak was located about 10kb downstream of the DPASE. Prior work revealed the ASE region to interact with the *Rag1* and *Rag2* promoters, but the downstream peak did not interact with any of these elements (8, 9). We focused further investigation on the DPASE.

Author Manuscript Author Manuscript Author Manuscript Author Manuscript

The DPASE controls RAG expression and locus conformation in DP thymocytes

To understand the role of the DPASE, we used CRISPR-Cas9 to generate a mouse model lacking 612 bp encompassing the accessible region (Fig. 1A and fig. S2A). Unlike ASE- or core ASE-deleted mice, which displayed severe loss of thymic cellularity (7, 9), DPASE-deleted mice displayed a small but reproducible increase in thymic cellularity and in the number of DP thymocytes compared to WT littermates (Figs. 1B and fig. S3A). However, there were no significant changes to the frequency with which DP thymocytes undergo positive selection, nor to the numbers of CD4SP and CD8SP thymocytes (Fig. 1, B and C, and fig. S3A). Thus, DPASE deletion caused no major block to thymocyte development.

We then measured RAG mRNA expression in DN3a and DP thymocytes from WT and DPASE-deleted mice by qPCR (Fig. 1D and fig. S3B). Consistent with previous data, we found *Rag1* and *Rag2* expression to be 3–5-fold higher in DP as compared to DN3a thymocytes of WT mice (Fig. 1D and fig. S1B). DN3a thymocytes of DPASE-deleted mice displayed expression of *Rag1* and *Rag2* that was indistinguishable from their WT counterparts. However, there were substantial reductions in *Rag1* and *Rag2* expression in DP thymocytes of DPASE-deleted mice, such that *Rag1* and *Rag2* were expressed in DP thymocytes at levels equivalent to those in DN thymocytes. Immunoblots revealed that ΔDPASE DP thymocytes expressed one-third to one-half as much RAG1 protein as their WT counterparts, whereas RAG2 protein was reduced modestly, if at all (Fig. 1E and fig. S3C). Thus, the DPASE upregulates RAG genes and proteins in DP thymocytes.

We previously established that the ASE acts as classical enhancer of *Rag1 and Rag2* promoter activity via long-distance interactions with the *Rag1* and *Rag2* promoters (8, 10). To understand if the DPASE contributes to the formation of enhancer-promoter interactions, we performed chromatin conformation capture (3C) in DP thymocytes using ASE and *Rag1* promoter viewpoints. WT DP thymocytes demonstrated interactions between the ASE and the *Rag1* and *Rag2* promoters, and between the *Rag1* and *Rag2* promoters. DP thymocytes lacking the DPASE displayed substantial reductions in all these interactions (Fig. 2A). ASE-promoter interactions increase the loading of RNA Pol II on the RAG promoters (8). To further address the role of the DPASE, we measured RNA Pol II occupancy at RAG locus *cis*-regulatory elements by chromatin immunoprecipitation (ChIP) using DP thymocytes from WT and DPASE-deleted mice. RNA Pol II loading was reduced at the core ASE and the *Rag1* promoter in the absence of the DPASE, whereas Pol II loading at the *Rag2* promoter remained unchanged (Fig. 2B). Further ChIP analysis detected no change in H3K4me3 at the *Rag1* and *Rag2* promoters in DPASE-deleted as compared to WT DP thymocytes (Fig. 2C). Thus, a basal level of RAG gene expression is established by the core ASE in DN thymocytes and the DPASE further enhances RAG expression in DP thymocytes by augmenting ASE-promoter contacts and RNA Pol II loading at the ASE and *Rag1* promoter.

DPASE-mediated RAG upregulation is essential to generate a complete *Tcra* repertoire

Because DP thymocytes of ASE-deleted mice expressed RAG genes without upregulation as compared to DN thymocytes, we could address the significance of this upregulation. To do so, we prepared 5’ Rapid Amplification of cDNA Ends (RACE) libraries from preselection

Author Manuscript Author Manuscript Author Manuscript Author Manuscript

DP thymocytes of WT and DPASE-deleted mice (Fig. S4A) and subjected them to high-throughput *Tcra* repertoire sequencing (17, 18). DP thymocytes undergo multiple cycles of *Tcra* rearrangement (19). Initial, or primary, Tcra rearrangements join Jα-proximal Vα gene segments to Vα-proximal Jα gene segments (Fig. S2B). Subsequent, or secondary, *Tcra* rearrangements can then replace the primary rearrangements by joining progressively more distal Vα gene segments to progressively more distal Jα gene segments, in a process that is terminated by either positive selection or cell death (19). This progression of proximal Vα-proximal Jα to central Vα-central Jα to distal Vα-distal Jα rearrangements creates a major diagonal in a two-dimensional plot of the combinatorial repertoire of WT DP thymocytes (Fig. 3A, left), as described previously (17, 20). In contrast, the combinatorial repertoire of DPASE-deleted littermates was more heavily biased towards proximal Vα-proximal Jα combinations (Fig. 3A, right). A focus on Jα usage frequencies in WT and DPASE-deleted littermates revealed relatively evenly distributed usage of proximal, central, and distal Jα segments in WT, with DPASE-deleted littermates displaying a 33% increase in usage of the 15 most proximal Jα segments, and a 40% reduction in usage of the 15 most distal Jα gene segments (Fig 3B, and table S1). These results suggest that DPASE-mediated upregulation of RAG gene expression in DP thymocytes is crucial to generate a complete *Tcra* repertoire.

We hypothesized that impaired usage of distal Vα-distal Jα combinations in DPASE-deleted mice reflected a slower rate of progression of secondary rearrangements across the Vα and Jα arrays. Alternatively, distal Vα and Jα gene segments could have an intrinsic requirement for elevated RAG expression for efficient rearrangement. To distinguish these possibilities, we used mice carrying *Tcrd*$^{\text{CreER}}$ and *Rosa26*$^{\text{fl-STOP-fl-ZsGreen}}$ alleles to measure *Tcra* rearrangement kinetics. Because *Tcrd* is expressed in DN thymocytes and is then deleted in DP thymocytes by *Tcra* rearrangement, only DN thymocytes will be labeled with ZsGreen immediately after tamoxifen injection. However, this cohort of ZsGreen^{+} DN thymocytes will then differentiate to and mature within the DP compartment, allowing their *Tcra* repertoire to be sampled over time (17, 21). We analyzed the *Tcra* repertoire in ZsGreen^{+} DP thymocytes isolated from WT and DPASE-deleted mice 24 h and 48 h after tamoxifen-induced labeling of DN thymocytes (Fig. S4B). As seen previously (17), WT ZsGreen^{+} DP thymocytes were heavily biased towards proximal Vα-proximal Jα combinations 24 h post-tamoxifen injection, but rearrangements were more broadly distributed at 48 h (Fig. 4A). In comparison to WT, DPASE-deleted DP thymocytes were more proximally biased at both time-points, with reduced usage of central Jα segments more prominent at 24 h, and reduced usage of distal Jα gene segments more prominent at 48 h (Fig. 4B, and table S1). These results indicate that reduced RAG expression in DP thymocytes causes delayed progression of secondary rearrangements all along the Vα and Jα arrays, rather than a selective loss of distal rearrangements.

To further support the evidence that RAG expression is limiting for *Tcra* repertoire formation, we analyzed Jα usage in DP thymocytes of mice with only a single functional allele of *Rag1* or *Rag2*. We used qPCR from genomic DNA to compare rearrangement of *Trav12* family members to various Jα segments in *Rag1*$^{+/+}$ versus *Rag1*$^{+/-}$ littermates, and in *Rag2*$^{+/+}$ versus *Rag2*$^{+/-}$ littermates. *Trav12* is useful for these assays because the multiple members of this gene family are distributed across the Vα array and rearrange broadly to proximal, central, and distal Jα gene segments. *Rag1*$^{+/-}$ DP thymocytes displayed reduced

Author Manuscript Author Manuscript Author Manuscript Author Manuscript

usage of distal Jα gene segments (Fig. S4C); *Rag2*$^{+/-}$ DP thymocytes trended similarly (Fig. S4D).

RORγt regulates RAG expression by binding to the DPASE

To investigate transcription factors that might regulate DPASE activity, we used JASPAR 2018 to identify predicted transcription factor binding sites (Fig. S5A). To narrow down potential candidates, we assessed the expression pattern of each of these transcription factors using the Immgen RNA-seq database, looking for factors displaying the highest expression and upregulation in DP thymocytes (Fig. S5B). We identified RAR-related orphan receptor γt (RORγt) (22) as a candidate regulator of the DPASE. The predicted binding site for RORγt displayed key nucleotides matching the ROR response element (RORE) consensus sequence (Fig. 5A). *Rorc* expression is substantially upregulated from DN to DP, and similar to RAG expression, is extinguished following positive selection (Fig. S1B). DP thymocytes lacking RORγt were shown to have modestly reduced RAG expression by semi-quantitative PCR (15), but the significance of that result was largely overlooked and the mechanism was not explored. To assess the role of the DPASE RORE, we used the RAG-expressing mouse DP thymocyte cell line VL3–3M2, which was previously used to characterize RAG locus regulation (8, 10). ChIP confirmed RORγt binding to the DPASE at a level comparable to that of the *Bcl2l1* promoter (Fig. 5B), a validated target of RORγt (14). We then used CRISPR-Cas9 to delete either the 612 bp DPASE or sequences of 28 and 30 bp spanning the DPASE RORE, on the two RAG alleles in VL3–3M2 cells (Fig. 5C and fig. S2A). RORγt binding was lost upon RORE deletion (Fig. 5D), and deletion of either the entire DPASE (Fig. 5E) or the RORE (Fig. 5F) resulted in substantial downregulation of *Rag1* and *Rag2* gene expression in these cells.

These results prompted us to further assess RORγt as a regulator of RAG gene expression in DP thymocytes *in vivo*. ChIP showed RORγt to bind to the DPASE in WT DP thymocytes (Fig. 5G). Moreover, qPCR revealed *Rag1* and *Rag2* expression to be reduced by 77–79% in DP thymocytes (Fig. 5H), but not DN thymocytes (Fig. 5I), of *Rorc(t)*$^{-/-}$ mice. We conclude that RORγt binds the DPASE to regulate RAG gene expression specifically in DP thymocytes.

RORγt regulates the *Tcra* repertoire via multiple pathways

RORγt-deficient mice have a defect in usage of distal Jα gene segments that was previously attributed to a DP thymocyte survival defect resulting from diminished expression of Bcl-xL (14, 15). The residual DP thymocytes of RORγt-deficient mice are also rapidly cycling (14), which may further suppress V(D)J recombination. The data reported herein reveal that RORγt influences the *Tcra* repertoire by supporting RAG gene expression. To better understand the relative contributions of various RORγt-dependent pathways to *Tcra* repertoire formation, we re-examined the *Tcra* repertoire defect in *Rorc(t)*$^{-/-}$ mice. Earlier characterization of the repertoire demonstrated impaired usage of distal Jα gene segments relative to proximal Jα segments in *Rorc*$^{-/-}$ DP thymocytes but did not directly compare rearrangement of individual Jα segments to WT (15). To obtain such data, we measured rearrangement of *Trav12* family members to various Jα segments in WT and *Rorc(t)*$^{-/-}$ DP thymocytes by qPCR of genomic DNA. This analysis revealed that rearrangement of central

Author Manuscript Author Manuscript Author Manuscript Author Manuscript

and distal Jα segments was reduced by several orders of magnitude in the absence of RORγt (Fig. 6A, left panel). By contrast, DPASE-deleted mice displayed a relatively modest defect in *Trav12* rearrangement that was limited to distal Jα segments (Fig. 6B, left panel). Because DPASE-deleted and *Rorc(t)*$^{-/-}$ mice have similar RAG expression defects (Fig. 1D and fig. 5H), much more dramatically impaired usage of central and distal Jα gene segments in the latter must result from other impacts of RORγ(t) deficiency, including increased cell cycling and reduced survival of DP thymocytes.

Notably, we also detected 77–96% reductions in the rearrangement of even the most proximal Jα gene segments (*Traj61*, *Traj58*, *Traj56*) in *Rorc(t)*$^{-/-}$ mice. (Fig. 6A, left panel). This seemed an unlikely consequence of reduced DP thymocyte survival but could reflect the dramatically different cell cycle status of WT and *Rorc(t)*$^{-/-}$ DP thymocytes. To analyze more comparable cell populations, we used CD71 staining to isolate highly cycling DP thymocytes of both genotypes (Fig. S6, A and B). These cells still displayed 76–83% reductions in rearrangements to the most proximal Jα segments in the absence of RORγt (Fig. 6A, right panel). However, no such reductions were detected in similar analyses of ΔDPASE mice (Fig. 6B, right panel), despite the fact that highly cycling *Rorc(t)*$^{-/-}$ and ΔDPASE DP thymocytes displayed comparable reductions in *Rag1* and *Rag2* expression (Fig. 6, C and D). Having ruled out cell survival, cell cycle status and RAG gene expression to explain defective proximal Jα rearrangement in *Rorc(t)*$^{-/-}$ DP thymocytes, we considered whether RORγt may also function as a direct regulator of the *Tcra* locus.

RORγt regulates the *Tcra* repertoire by direct binding to *Tcra* locus chromatin

High quality RORγt ChIP-seq datasets are available for Th17 cells but not DP thymocytes. Th17 cells, however, should be variably deleted for *Tcra* locus chromatin through *Traj2*, due to the presence of heterogeneous Vα-to-Jα rearrangements on both alleles. Focusing on the fully represented region downstream of *Traj2*, in two independent data sets (23, 24) we identified a major peak of RORγt binding associated with the *Tcra* enhancer (Eα), and several less prominent peaks both upstream and downstream of Eα (Fig. S7, A and B). We noted, as well, a minor peak associated with the T early alpha (TEA) promoter, the major promoter of germline transcripts across the Jα array (25, 26). Although barely detectable, this binding could be meaningful, because TEA chromatin should be vastly underrepresented due to its deletion on both alleles in the majority of peripheral T cells. In addition, prior work had shown RORγt to bind to the TEA promoter *in vitro* (27).

To quantitatively assess RORγt binding to *Tcra* locus chromatin in DP thymocytes *in vivo*, we injected *Rag2*$^{-/-}$ mice with anti-CD3ε to induce DN to DP differentiation, and prepared chromatin from thymocytes in which the *Tcra* locus was held in germline configuration. This analysis revealed strong binding of RORγt to both TEA and Eα (Fig. 7A). JASPAR TF motif analysis identified two overlapping, conserved ROREs immediately upstream of, but separated from, the Tα1 protein binding region of Eα (28). To further establish RORγt as a direct regulator of the *Tcra* repertoire, we used CRISPR-Cas9 to generate mice lacking these ROREs (Eα$^{\Delta RORE}$) (Fig. 7B and fig. S2B). ChIP confirmed that RORγt binding to Eα was lost in Eα$^{\Delta RORE}$ DP thymocytes (Fig. 7C). Unlike Eα-deleted mice, which are blocked at the DP stage of thymocyte development (29), Eα$^{\Delta RORE}$ mice displayed normal thymic

Author Manuscript Author Manuscript Author Manuscript Author Manuscript

cellularity with no obvious developmental block (Fig. 7D and fig. S7C). However, there were 32–41% reductions in *Trav12* rearrangements to central and distal Jα gene segments (Fig. 7E), indicating that RORγt regulates the *Tcra* repertoire, in part, by direct binding to *Tcra* locus chromatin. We detected no effect of the mutation on *Tcra* germline transcription (Fig. 7F).

Discussion

Here we have demonstrated that DP thymocytes display a unique requirement for high level RAG gene expression that is generated by cooperation of two distinct modules of the RAG ASE. One module, the core ASE, is responsible for a baseline level of RAG gene expression in both DN3a and DP thymocytes. The second module, the DPASE, is specifically required to upregulate RAG gene expression in DP thymocytes. Without this boost to RAG gene expression, DP thymocytes display a defect in secondary Vα-Jα recombination and are incapable of generating a replete *Tcra* repertoire. We further showed that DPASE-mediated upregulation of RAG gene expression depends on RORγt, a transcription factor that is highly expressed in DP thymocytes. We also reveal a direct role of RORγt in regulating *Tcra* recombination by binding to Eα. Previous studies showed that RORγt promotes secondary *Tcra* rearrangement by upregulating Bcl-xL to maintain DP thymocyte lifespan (14, 15). RORγt was also shown to upregulate p27 to promote G1 cell-cycle arrest (14), which would shield RAG2 from cell-cycle-mediated degradation (30, 31). These and our current results reveal RORγt to act as a multi-faceted regulator of the *Tcra* repertoire.

An important conclusion from our work is that RAG levels sufficient to support the recombination programs of the *Tcrb*, *Tcrg* and *Tcrd* loci in DN thymocytes are insufficient to fully support *Tcra* recombination in DP thymocytes. Hierarchical requirements for RAG protein abundance were also revealed by complete ASE deletion, in which case low level RAG expression driven by residual RAG promoter activity could support some Vγ-Jγ, Vδ-Dδ-Jδ, and Dβ-Jβ rearrangement, but little Vβ-DβJβ rearrangement (9). We suggest that RAG expression is normally limiting for V(D)J recombination *in vivo*, and that RAG expression levels are fine-tuned to meet the needs of the recombination programs at different developmental stages. For example, *Tcrb*, *Tcrg* and *Tcrd* rearrangements are thought to occur in the same DN2 and DN3 thymocytes, with the outcome of rearrangements influencing αβ/γδ lineage choice (32–36). As well, competition between two *Tcrb* alleles presenting relatively inefficient substrates for RAG is thought to contribute to *Tcrb* allelic exclusion (37, 38). The competitive nature of these recombination programs may be enhanced by lower levels of RAG gene expression in DN thymocytes. In contrast, in DP thymocytes, both *Tcra* alleles typically undergo multiple cycles of Vα-to-Jα rearrangement over the course of 3–4 days to fully sample the Vα and Jα arrays and facilitate positive selection. We believe that a recombination program requiring multiple cycles of RAG binding, Vα-Jα synapsis, DNA cleavage, and rejoining will be facilitated by elevated RAG expression that ensures efficient RAG loading onto newly generated VαJα recombination centers during each cycle of rearrangement. With this in mind, we note that *Rag1* and *Rag2* mRNA half-lives have been estimated to be in the range of 40 min (39, 40), and that whereas RAG2 protein is quite stable in non-cycling cells, RAG1 is rapidly degraded with a half-life of only 10–30 min (40–43). Mouse thymocytes, which are primarily DP, were

Author Manuscript Author Manuscript Author Manuscript Author Manuscript

shown to contain only about 1000 RAG1 dimers per cell, with about a seven-fold molar excess of RAG2 (44). Given that both RAG proteins are distributed over thousands of sites genome-wide (2), and that some RAG1 may localize to the nucleolus (45), the abundance of RAG proteins, and in particular the abundance of RAG1, could well be limiting for the pace of *Tcra* rearrangements in DP thymocytes. This would explain why a relatively modest and selective reduction in RAG1 protein expression translates to reduced kinetics of secondary *Tcra* recombination in ΔDPASE DP thymocytes. In further support of this idea, we detected defects in *Tcra* rearrangement in *Rag1*$^{+/-}$, and even in *Rag2*$^{+/-}$, DP thymocytes. Similarly, prior work revealed *Rag1*$^{+/-}$ B cells to display reduced immunoglobulin light chain receptor editing (39), whereas B cells with stabilized RAG1 protein displayed increased editing (43). Although elevated RAG expression in DP thymocytes may suit the *Tcra* recombination program, it may come at a cost, since ΔDPASE mice displayed a modest, but reproducible, increase in the number of DP thymocytes. We suspect that elevated RAG expression in WT DP thymocytes may pose an increased threat to genome integrity (2), with elevated cell death impacting the size of the DP population. This tradeoff may set an upper limit to physiologically useful RAG gene expression. Although the increase in DP thymocytes might alternatively be explained by impaired positive selection, we detected no change in the frequency of DP thymocytes undergoing positive selection in ΔDPASE mice.

Although the core ASE sequence is highly conserved in reptiles, birds and mammals, DPASE conservation is primarily restricted to mammals (9). This suggests that a functional DPASE represents a relatively recent adaptation to boost RAG expression and expand the *Tcra* repertoire. Analysis of ASE region chromatin signatures in human thymocyte subsets revealed the core ASE to display an active enhancer chromatin signature in CD34^{+} DN and early cortical DP thymocytes, whereas the DPASE displayed a poised enhancer signature in the former and an active enhancer signature in the latter (46) (Fig. S8). Thus, DPASE-mediated RAG gene regulation appears to be conserved between mouse and human thymocytes.

RORγt was identified as an important regulator of the *Tcra* repertoire because it supports expression of the anti-apoptotic protein Bcl-xL and maintains DP thymocyte survival (14, 15). Because the observed defect in distal Jα usage in RORγt-deficient mice could be complemented by overexpression of Bcl-xL, it was assumed that RORγt regulated the *Tcra* repertoire solely by prolonging DP thymocyte survival (15). However, Bcl-xL overexpression did not simply normalize the *Tcra* repertoire; rather, it generated a repertoire that was heavily biased to the most distal Jα gene segments, presumably because it extended DP thymocyte lifespan well beyond what is physiologically normal. This could have compensated for influences of RORγt on the *Tcra* repertoire that are unrelated to lifespan per se. Our current work adds to this picture by demonstrating quantitative defects in RAG gene expression and in proximal Jα rearrangements in *Rorc(t)*$^{-/-}$ DP thymocytes. Thus we now believe that RORγt regulates the *Tcra* repertoire through multiple pathways. First, it orchestrates a critical upregulation of RAG protein expression, due to in part to DPASE-dependent augmentation of *Rag1* and *Rag2* transcription, and in part to stabilization of RAG2 protein by p27-dependent cell-cycle arrest (14). Second, it helps ready the *Tcra* locus as an efficient substrate for Vα-Jα rearrangement by binding to Eα. Third, it allows

Author Manuscript Author Manuscript Author Manuscript Author Manuscript

the Vα and Jα arrays to be fully sampled by RAG proteins by keeping thymocytes alive for the requisite 3–4 days (15).

An important limitation of our work is that we do not yet fully understand the direct effects of RORγt on *Tcra* locus chromatin. We show here that deletion of an Eα RORE diminishes the contribution of distal Jα segments to the *Tcra* repertoire. However, loss of Eα RORγt binding cannot explain the quite substantial disruption of proximal Jα rearrangement in *Rorc(t)*$^{-/-}$ mice. Rather, we suspect that the defect in proximal Jα rearrangement may primarily reflect loss of RORγt binding at the TEA promoter RORE. We note, however, that this RORE can have no direct influence on secondary Vα-Jα rearrangements because the TEA promoter is deleted by primary rearrangement. This leads us to suggest that the Eα RORE may function redundantly with the TEA RORE before primary rearrangement, but may then contribute in non-redundant fashion once the TEA promoter is deleted, thus explaining the selective defect in central and distal Jα usage in Eα RORE-deleted mice. It will be interesting to further test the proposed division of labor between these two *Tcra* locus ROREs in future experiments.

Materials and Methods

Study design

The aims of this study were to determine the mechanism and biological significance of elevated RAG gene expression in DP thymocytes. To accomplish these aims we generated mice with deletion of a RAG locus element (DPASE) that displays DP thymocyte-specific chromatin accessibility. Flow cytometry, qRT-PCR, immunoblots, ChIP and 3C were used to evaluate the effects of this deletion on RAG locus function. 5'RACE and deep sequencing were used to assess effects on the *Tcra* repertoire. To investigate the role of RORγt as a regulator of DPASE function, we created a mutation in the DPASE RORE of mouse DP thymocyte cell line VL3–3M2 and used ChIP and qRT-PCR for analysis, and we analyzed *Tcra* rearrangement by quantitative genomic PCR in DP thymocytes of *Rorc(t)*$^{-/-}$ mice. Then, to determine whether RORγt also regulates *Tcra* rearrangement by direct binding to the *Tcra* locus, we generated mice lacking a *Tcra* enhancer RORE, and used flow cytometry, ChIP, quantitative genomic PCR and qRT-PCR to evaluate effects of the mutation on *Tcra* locus function. Mouse experiments compared littermate controls. Generally, three or more biological replicates were analyzed in each experiment; details are provided in the figure legends. Experiments were performed without blinding. No data was excluded from analysis.

Mice

ΔDPASE and Eα$^{\Delta RORE}$ mice were generated by CRISPR/Cas9 genome editing by the Duke University Transgenic and Knockout Mouse Shared Resource. Guide RNAs with predicted high specificity and cleavage efficiency were designed using the UCSC genome browser CRISPR/Cas9-NGG target feature. ΔDPASE mice were generated by two guide-mediated CRISPR/Cas9 targeting of C57BL/6J embryos. Mice with a deleted DPASE region (mm10 Chr2: 101,552,279 to 101, 552, 890) were identified by PCR and Sanger sequencing, were bred to C57BL/6J, and progeny were intercrossed to generate littermate WT and ΔDPASE

Author Manuscript Author Manuscript Author Manuscript Author Manuscript

mice. RAG gene expression changes were similar in progeny of two founders carrying the same deletion; results are combined in Fig. 1C. For TCR repertoire analysis, ΔDPASE mice were bred to *Tcrd*$^{CreER/CreER}$*Rosa26*$^{ZsG/ZsG}$ mice, which carry modified strain 129 *Tcra-Tcrd* alleles on a C57BL/6J genetic background (21). *Tcrd*$^{CreER/CreER}$*Rosa26*$^{ZsG/ZsG}$ littermates segregating WT and ΔDPASE alleles at the RAG locus were used for 5' RACE. Eα$^{\Delta RORE}$ mice were generated by CRISPR/Cas9 targeting of F1 embryos generated through breeding of strain 129 male and C57BL/6J female mice. Single guide-mediated CRISPR/Cas9 was used to mutate two overlapping ROREs at Eα (mm10 Chr14: 54,227,367–54,227,386). Screening by PCR and Sanger sequencing identified a 10 bp deletion on the 129 allele (mm10 Chr14: 54,227,375– 54,227,384). Founders were bred to 129 and progeny were intercrossed to generate WT and Eα$^{\Delta RORE}$ littermates for analysis. *Rorc(t)*$^{-/-}$ (also known as *Rorc(t)*^{GFP}) mice (47) were a kind gift from Maria Ciofani (Duke University). *Rorc(t)*$^{-/-}$ mice and Eα$^{\Delta RORE}$ mice were bred with *Rag2*$^{-/-}$ mice to analyze germline transcription on a recombinase-deficient background. *Rag1*$^{-/-}$ and *Rag2*$^{-/-}$ mice were crossed with C57BL/6J and F1 progeny were crossed again to C57BL/6J to analyze *Rag1* and *Rag2* dosage effects. Mice were used for experiments at 4–6 weeks of age unless otherwise noted. All mice were housed in a specific pathogen-free facility managed by the Duke University Division of Laboratory Animal Resources and were used in accord with protocols approved by the Duke University Institutional Animal Care and Use Committee. Mice of both genders were included in all experiments and no differences were noted. CRISPR guide sequences are listed in Table S2.

Flow cytometry and cell sorting

All antibodies and reagents were purchased from BioLegend, unless stated otherwise. For analysis of total thymocytes or isolation of preselection DP thymocytes ($CD4^+CD8^+Lin^-CD3^{lo}7AAD^-$), total thymocytes were stained with anti-CD4 (GK1.5), anti-CD8α (53–6.7), anti-CD3ε (145–2C11), 7-aminoactinomycin D (7AAD), and PE-Cy5–conjugated lineage (Lin) markers anti-B220 (RA3–6B2), anti-CD11b (M1/70), anti-CD11c (N418), anti-F4/80 (BM8), anti–Gr-1 (RB6–8C5), and anti–Ter-119 (TER-119). To assess positive selection ($CD4^+CD8^+CD5^+CD69^+$), staining included anti-CD5 (53–7.3) and anti-CD69 (H1.2F3). To obtain early DP thymocytes ($CD4^+CD8^+CD71^+Lin^-CD3^{lo}7AAD^-$), staining included anti-CD71 (R17217). DN3a thymocytes ($Lin^-CD25^+CD44^-CD28^-$) were isolated by staining with anti-CD25 (3C7), anti-CD44 (IM7), anti-CD28 (37.51), and lineage markers. To isolate DP thymocytes from *Rag2*$^{-/-}$ mice, mice were injected i.p. with 150 μg anti-CD3ε and sacrificed ten days later. To isolate $ZsGreen^+$ preselection DP thymocytes, *Tcrd*$^{CreER/CreER}$ *Rosa26*$^{ZsG/ZsG}$ *mice* were injected i.p. with 100 μl of 10 mg/ml tamoxifen (Sigma-Aldrich) in corn oil and were sacrificed 24 or 48 h later.

Cell cycle analysis

Ten million thymocytes were stained with 1:200 (vol/vol) Zombie Aqua™ viability dye (BioLegend) for 15 min at 23°C in the dark, were washed once, and then stained with antibodies for 15 min on ice in the dark. Cells were then washed and crosslinked in the presence of 1% (vol/vol) paraformaldehyde for 10 min on ice. Crosslinked cells were washed and resuspended in cell staining buffer containing 25 ug/ml propidium iodide (BioLegend) and 1 ug/ml RNaseA for 15 min. Cell cycle analysis was performed using

Author Manuscript Author Manuscript Author Manuscript Author Manuscript

a LSRFortessa Cell Analyzer (BD Biosciences). The G_0/G_1 gate was set by the propidium iodide staining profile of total DP thymocytes.

Quantitative RT-PCR

TRIzol reagent (Invitrogen) was used to isolate total cellular RNA as per manufacturer's instructions. For cDNA synthesis, 1 ug of RNA was subjected to DNase I treatment (Invitrogen) and IScript-mediated reverse transcription (Biorad) according to the manufacturer's instructions. Levels of *Actb*, *Rag1*, *Rag2*, *Hprt*, TEA, *Traj56*, *Traj31*, and *Trac* transcripts were measured by SYBR Green qPCR (Qiagen) as described (8, 48). Primers are listed in Table S2.

Immunoblot

Purified DP thymocyte or unfractionated control tissue sample extracts (2×10^6 cell equivalents of each) were electrophoresed through 7.5% sodium dodecyl sulfate polyacrylamide gels, transferred to polyvinylidene difluoride membranes, and incubated with anti-Rag1 #23 (1:1000), anti-Rag2 (1:500) (49), or anti-β-actin (BioLegend), followed by goat anti-rabbit-horseradish peroxidase (Jackson ImmunoResearch) or rabbit anti-rat-horseradish peroxidase (Jackson ImmunoResearch). Blots were developed using ECL PRIME (Cytiva) and imaged using a Bio-Rad ChemiDoc MP.

Chromosome conformation capture (3C)

3C was initiated by crosslinking 10^7 thymocytes with 2% (vol/vol) paraformaldehyde for 10 min at 23°C, and was otherwise carried out as described (10). Final ligated products were quantified by qPCR by using BglII-digested and ligated bacterial artificial chromosomes 374F10 and 241E7 and PCR primers and Taqman PCR probes as described (8). Primers are listed in Table S2.

Tcra repertoire analysis

The *Tcra* repertoire was determined by 5' RACE and deep sequencing as described (17, 18, 20). cDNA was synthesized from 700 ng of total RNA extracted from either preselection DP thymocytes or $ZsGreen^+$ preselection DP thymocytes using Superscript II (Invitrogen) and was amplified using a KAPA HiFi HotStart PCR Kit (Roche). Analysis was performed using MiXCR as described (17, 18, 20).

CRISPR/Cas9 targeting of VL3–3M2 cells

The mouse VL3–3M2 cell line (50) was cultured as described (10). Two guide-mediated CRISPR/Cas9 was used to delete the DPASE region (mm10 Chr2: 101,552,279 to 101, 552, 890) or the DPASE RORE (mm10 Chr2: 101,552,595 to 101, 552, 624). Guide sequences are listed in Table S2. Guide sequences were cloned into pX458 (Addgene). Transfection of VL3–3M2 cells and isolation of transfected clones were performed as described (10). Mutant clones were identified by genomic DNA PCR and sequencing.

Author Manuscript Author Manuscript Author Manuscript Author Manuscript

Chromatin Immunoprecipitation (ChIP)

ChIP was performed as described (10), with several modifications. 10^7 DP thymocytes or VL3–3M2 cells were subjected to formaldehyde crosslinking. Following cell lysis, nuclei were pelleted and lysed in 100 μl of 50 mM Tris-HCl pH 8, 10 mM EDTA, 1% (wt/vol) SDS, 0.1 M benzamidine and 0.1 M PMSF for 10 min at 23°C, after which chromatin was diluted to 1 ml with 0.01% (wt/vol) SDS, 1.1% (vol/vol) Triton X-100, 1.2 mM EDTA, 16.7 mM Tris-HCl pH8, 167 mM NaCl. ChIP samples were analyzed by SYBR-green qPCR as described (8). RORγt ChIP signals were expressed as % bound (bound/input X 100) or as relative enrichment (bound/input relative to that for nonspecific IgG control). Pol II and H3K4me3 ChIP signals were expressed as relative enrichment (bound/input relative to that for the *B2m* promoter), as described (8). Primers are listed in Table S2.

Tcra recombination in genomic DNA

Trav12 family to Jα rearrangements in genomic DNA prepared from preselection DP or $CD71^+$ early DP thymocytes were analyzed by SYBR-green qPCR as described (51). Primers are listed in Table S2.

Statistical analysis

Data were analyzed by unpaired t-test or two-way ANOVA with Holm-Sidak's correction for multiple comparison, using GraphPad Prism version 6.07 for Windows. The number of biological replicates, the method used for data normalization, and the statistical test used for each experiment is provided in the figure legend. Results are generally reported as the mean and s.e.m. The mean and individual data points are presented for flow cytometry experiments. *P* values are reported as follows in all experiments: **P*<0.05, ***P*<0.01, ****P*<0.001, *****P*<0.0001.

Supplementary Material

Refer to Web version on PubMed Central for supplementary material.

Acknowledgments:

We thank C. Bock and G. Kucera of the Duke Transgenic Mouse Facility for production of mice by gene targeting; J. Mohammed, L. Martinek, N. Martin, and B. Li of the Duke Flow Cytometry Facility for help with cell sorting and analysis; and Y. Zhuang and M. Ciofani for helpful comments on the manuscript.

Funding:

Supported by the US National Institutes of Health (R35 GM136284 to M.S.K. and RO1 AI032524 to D.G.S.).

References and Notes:

1. Schatz DG, Spanopoulou E, Biochemistry of V(D)J recombination. Curr Top Microbiol Immunol 290, 49–85 (2005). [PubMed: 16480039]
2. Teng G, Maman Y, Resch W, Kim M, Yamane A, Qian J, Kieffer-Kwon KR, Mandal M, Ji Y, Meffre E, Clark MR, Cowell LG, Casellas R, Schatz DG, RAG Represents a Widespread Threat to the Lymphocyte Genome. Cell 162, 751–765 (2015). [PubMed: 26234156]
3. Kuo TC, Schlissel MS, Mechanisms controlling expression of the RAG locus during lymphocyte development. Curr Opin Immunol 21, 173–178 (2009). [PubMed: 19359154]

Author Manuscript Author Manuscript Author Manuscript Author Manuscript

4. Wayne J, Suh H, Misulovin Z, Sokol KA, Inaba K, Nussenzweig MC, A regulatory role for recombinase activating genes, RAG-1 and RAG-2, in T cell development. Immunity 1, 95–107 (1994). [PubMed: 7534201]
5. Barreto V, Marques R, Demengeot J, Early death and severe lymphopenia caused by ubiquitous expression of the Rag1 and Rag2 genes in mice. Eur J Immunol 31, 3763–3772 (2001). [PubMed: 11745397]
6. Miyazaki K, Miyazaki M, The Interplay Between Chromatin Architecture and Lineage-Specific Transcription Factors and the Regulation of Rag Gene Expression. Front Immunol 12, 659761 (2021). [PubMed: 33796120]
7. Yannoutsos N, Barreto V, Misulovin Z, Gazumyan A, Yu W, Rajewsky N, Peixoto BR, Eisenreich T, Nussenzweig MC, A cis element in the recombination activating gene locus regulates gene expression by counteracting a distant silencer. Nat Immunol 5, 443–450 (2004). [PubMed: 15021880]
8. Hao B, Naik AK, Watanabe A, Tanaka H, Chen L, Richards HW, Kondo M, Taniuchi I, Kohwi Y, Kohwi-Shigematsu T, Krangel MS, An anti-silencer- and SATB1-dependent chromatin hub regulates Rag1 and Rag2 gene expression during thymocyte development. J Exp Med 212, 809–824 (2015). [PubMed: 25847946]
9. Miyazaki K, Watanabe H, Yoshikawa G, Chen K, Hidaka R, Aitani Y, Osawa K, Takeda R, Ochi Y, Tani-Ichi S, Uehata T, Takeuchi O, Ikuta K, Ogawa S, Kondoh G, Lin YC, Ogata H, Miyazaki M, The transcription factor E2A activates multiple enhancers that drive Rag expression in developing T and B cells. Sci Immunol 5, (2020).
10. Naik AK, Byrd AT, Lucander ACK, Krangel MS, Hierarchical assembly and disassembly of a transcriptionally active RAG locus in CD4(+)CD8(+) thymocytes. J Exp Med 216, 231–243 (2019). [PubMed: 30545902]
11. Yoshida H, Lareau CA, Ramirez RN, Rose SA, Maier B, Wroblewska A, Desland F, Chudnovskiy A, Mortha A, Dominguez C, Tellier J, Kim E, Dwyer D, Shinton S, Nabekura T, Qi Y, Yu B, Robinette M, Kim KW, Wagers A, Rhoads A, Nutt SL, Brown BD, Mostafavi S, Buenrostro JD, Benoist C, Immunological Genome P, The cis-Regulatory Atlas of the Mouse Immune System. Cell 176, 897–912 e820 (2019). [PubMed: 30686579]
12. Feng D, Chen Y, Dai R, Bian S, Xue W, Zhu Y, Li Z, Yang Y, Zhang Y, Zhang J, Bai J, Qin L, Kohwi Y, Shi W, Kohwi-Shigematsu T, Ma J, Liao S, Hao B, Chromatin organizer SATB1 controls the cell identity of CD4(+) CD8(+) double-positive thymocytes by regulating the activity of super-enhancers. Nat Commun 13, 5554 (2022). [PubMed: 36138028]
13. Zelenka T, Klonizakis A, Tsoukatou D, Papamatheakis DA, Franzenburg S, Tzerpos P, Tzonevrakis IR, Papadogkonas G, Kapsetaki M, Nikolaou C, Plewczynski D, Spilianakis C, The 3D enhancer network of the developing T cell genome is shaped by SATB1. Nat Commun 13, 6954 (2022). [PubMed: 36376298]
14. Sun Z, Unutmaz D, Zou YR, Sunshine MJ, Pierani A, Brenner-Morton S, Mebius RE, Littman DR, Requirement for RORgamma in thymocyte survival and lymphoid organ development. Science 288, 2369–2373 (2000). [PubMed: 10875923]
15. Guo J, Hawwari A, Li H, Sun Z, Mahanta SK, Littman DR, Krangel MS, He YW, Regulation of the TCRalpha repertoire by the survival window of CD4(+)CD8(+) thymocytes. Nat Immunol 3, 469–476 (2002). [PubMed: 11967541]
16. Hosoya T, D'Oliveira Albanus R, Hensley J, Myers G, Kyono Y, Kitzman J, Parker SCJ, Engel JD, Global dynamics of stage-specific transcription factor binding during thymocyte development. Sci Rep 8, 5605 (2018). [PubMed: 29618724]
17. Carico ZM, Roy Choudhury K, Zhang B, Zhuang Y, Krangel MS, Tcrd Rearrangement Redirects a Processive Tcra Recombination Program to Expand the Tcra Repertoire. Cell reports 19, 2157–2173 (2017). [PubMed: 28591585]
18. Dauphars DJ, Wu G, Bassing CH, Krangel MS, Methods for Study of Mouse T Cell Receptor alpha and beta Gene Rearrangements. Methods Mol Biol 2580, 261–282 (2023). [PubMed: 36374463]
19. Carico Z, Krangel MS, Chromatin Dynamics and the Development of the TCRalpha and TCRdelta Repertoires. Adv Immunol 128, 307–361 (2015). [PubMed: 26477370]

Author Manuscript Author Manuscript Author Manuscript Author Manuscript

20. Dauphars DJ, Mihai A, Wang L, Zhuang Y, Krangel MS, Trav15-dv6 family Tcrd rearrangements diversify the Tcra repertoire. J Exp Med 219, (2022).
21. Zhang B, Wu J, Jiao Y, Bock C, Dai M, Chen B, Chao N, Zhang W, Zhuang Y, Differential Requirements of TCR Signaling in Homeostatic Maintenance and Function of Dendritic Epidermal T Cells. J Immunol 195, 4282–4291 (2015). [PubMed: 26408667]
22. Jetten AM, Takeda Y, Slominski A, Kang HS, Retinoic acid-related Orphan Receptor gamma (RORgamma): connecting sterol metabolism to regulation of the immune system and autoimmune disease. Curr Opin Toxicol 8, 66–80 (2018). [PubMed: 29568812]
23. Ciofani M, Madar A, Galan C, Sellars M, Mace K, Pauli F, Agarwal A, Huang W, Parkhurst CN, Muratet M, Newberry KM, Meadows S, Greenfield A, Yang Y, Jain P, Kirigin FK, Birchmeier C, Wagner EF, Murphy KM, Myers RM, Bonneau R, Littman DR, A validated regulatory network for Th17 cell specification. Cell 151, 289–303 (2012). [PubMed: 23021777]
24. Xiao S, Yosef N, Yang J, Wang Y, Zhou L, Zhu C, Wu C, Baloglu E, Schmidt D, Ramesh R, Lobera M, Sundrud MS, Tsai PY, Xiang Z, Wang J, Xu Y, Lin X, Kretschmer K, Rahl PB, Young RA, Zhong Z, Hafler DA, Regev A, Ghosh S, Marson A, Kuchroo VK, Small-molecule RORgammat antagonists inhibit T helper 17 cell transcriptional network by divergent mechanisms. Immunity 40, 477–489 (2014). [PubMed: 24745332]
25. Villey I, Caillol D, Selz F, Ferrier P, de Villartay JP, Defect in rearrangement of the most 5' TCR-J alpha following targeted deletion of T early alpha (TEA): implications for TCR alpha locus accessibility. Immunity 5, 331–342 (1996). [PubMed: 8885866]
26. Villey I, Quartier P, Selz F, de Villartay JP, Germ-line transcription and methylation status of the TCR-J alpha locus in its accessible configuration. Eur J Immunol 27, 1619–1625 (1997). [PubMed: 9247569]
27. Villey I, de Chasseval R, de Villartay JP, RORgammaT, a thymus-specific isoform of the orphan nuclear receptor RORgamma / TOR, is up-regulated by signaling through the pre-T cell receptor and binds to the TEA promoter. Eur J Immunol 29, 4072–4080 (1999). [PubMed: 10602018]
28. Hernandez-Munain C, Sleckman BP, Krangel MS, A developmental switch from TCR delta enhancer to TCR alpha enhancer function during thymocyte maturation. Immunity 10, 723–733 (1999). [PubMed: 10403647]
29. Sleckman BP, Bardon CG, Ferrini R, Davidson L, Alt FW, Function of the TCR alpha enhancer in alphabeta and gammadelta T cells. Immunity 7, 505–515 (1997). [PubMed: 9354471]
30. Lin WC, Desiderio S, Cell cycle regulation of V(D)J recombination-activating protein RAG-2. Proc Natl Acad Sci U S A 91, 2733–2737 (1994). [PubMed: 8146183]
31. Lee J, Desiderio S, Cyclin A/CDK2 regulates V(D)J recombination by coordinating RAG-2 accumulation and DNA repair. Immunity 11, 771–781 (1999). [PubMed: 10626899]
32. Livak F, Petrie HT, Crispe IN, Schatz DG, In-frame TCR delta gene rearrangements play a critical role in the alpha beta/gamma delta T cell lineage decision. Immunity 2, 617–627 (1995). [PubMed: 7796295]
33. Capone M, Hockett RD Jr., Zlotnik A, Kinetics of T cell receptor beta, gamma, and delta rearrangements during adult thymic development: T cell receptor rearrangements are present in CD44(+)CD25(+) Pro-T thymocytes. Proc Natl Acad Sci U S A 95, 12522–12527 (1998). [PubMed: 9770518]
34. Livak F, Tourigny M, Schatz DG, Petrie HT, Characterization of TCR gene rearrangements during adult murine T cell development. J Immunol 162, 2575–2580 (1999). [PubMed: 10072498]
35. Aifantis I, Azogui O, Feinberg J, Saint-Ruf C, Buer J, von Boehmer H, On the role of the pre-T cell receptor in alphabeta versus gammadelta T lineage commitment. Immunity 9, 649–655 (1998). [PubMed: 9846486]
36. Ciofani M, Zuniga-Pflucker JC, Determining gammadelta versus alphass T cell development. Nat Rev Immunol 10, 657–663 (2010). [PubMed: 20725107]
37. Wu GS, Yang-Iott KS, Klink MA, Hayer KE, Lee KD, Bassing CH, Poor quality Vbeta recombination signal sequences stochastically enforce TCRbeta allelic exclusion. J Exp Med 217, (2020).
38. Wu GS, Bassing CH, Inefficient V(D)J recombination underlies monogenic T cell receptor beta expression. Proc Natl Acad Sci U S A 117, 18172–18174 (2020). [PubMed: 32690689]

Author Manuscript Author Manuscript Author Manuscript Author Manuscript

39. Verkoczy L, Ait-Azzouzene D, Skog P, Martensson A, Lang J, Duong B, Nemazee D, A role for nuclear factor kappa B/rel transcription factors in the regulation of the recombinase activator genes. Immunity 22, 519–531 (2005). [PubMed: 15845455]
40. Fisher MR, Rivera-Reyes A, Bloch NB, Schatz DG, Bassing CH, Immature Lymphocytes Inhibit Rag1 and Rag2 Transcription and V(D)J Recombination in Response to DNA Double-Strand Breaks. J Immunol 198, 2943–2956 (2017). [PubMed: 28213501]
41. Grawunder U, Schatz DG, Leu TM, Rolink A, Melchers F, The half-life of RAG-1 protein in precursor B cells is increased in the absence of RAG-2 expression. J Exp Med 183, 1731–1737 (1996). [PubMed: 8666930]
42. Ochodnicka-Mackovicova K, Bahjat M, Maas C, van der Veen A, Bloedjes TA, de Bruin AM, van Andel H, Schrader CE, Hendriks RW, Verhoeyen E, Bende RJ, van Noesel CJ, Guikema JE, The DNA Damage Response Regulates RAG1/2 Expression in Pre-B Cells through ATM-FOXO1 Signaling. J Immunol 197, 2918–2929 (2016). [PubMed: 27559048]
43. Schabla NM, Perry GA, Palmer VL, Swanson PC, VprBP (DCAF1) Regulates RAG1 Expression Independently of Dicer by Mediating RAG1 Degradation. J Immunol 201, 930–939 (2018). [PubMed: 29925675]
44. Zhang YH, Shetty K, Surleac MD, Petrescu AJ, Schatz DG, Mapping and Quantitation of the Interaction between the Recombination Activating Gene Proteins RAG1 and RAG2. J Biol Chem 290, 11802–11817 (2015). [PubMed: 25745109]
45. Brecht RM, Liu CC, Beilinson HA, Khitun A, Slavoff SA, Schatz DG, Nucleolar localization of RAG1 modulates V(D)J recombination activity. Proc Natl Acad Sci U S A 117, 4300–4309 (2020). [PubMed: 32047031]
46. Cieslak A, Charbonnier G, Tesio M, Mathieu EL, Belhocine M, Touzart A, Smith C, Hypolite G, Andrieu GP, Martens JHA, Janssen-Megens E, Gut M, Gut I, Boissel N, Petit A, Puthier D, Macintyre E, Stunnenberg HG, Spicuglia S, Asnafi V, Blueprint of human thymopoiesis reveals molecular mechanisms of stage-specific TCR enhancer activation. J Exp Med 217, (2020).
47. Eberl G, Littman DR, Thymic origin of intestinal alphabeta T cells revealed by fate mapping of RORgammat+ cells. Science 305, 248–251 (2004). [PubMed: 15247480]
48. Zhao H, Li Z, Zhu Y, Bian S, Zhang Y, Qin L, Naik AK, He J, Zhang Z, Krangel MS, Hao B, A role of the CTCF binding site at enhancer Ealpha in the dynamic chromatin organization of the Tcra-Tcrd locus. Nucleic Acids Res 48, 9621–9636 (2020). [PubMed: 32853367]
49. Coster G, Gold A, Chen D, Schatz DG, Goldberg M, A dual interaction between the DNA damage response protein MDC1 and the RAG1 subunit of the V(D)J recombinase. J Biol Chem 287, 36488–36498 (2012). [PubMed: 22942284]
50. Groves T, Katis P, Madden Z, Manickam K, Ramsden D, Wu G, Guidos CJ, In vitro maturation of clonal CD4+CD8+ cell lines in response to TCR engagement. J Immunol 154, 5011–5022 (1995). [PubMed: 7730608]
51. Shih HY, Verma-Gaur J, Torkamani A, Feeney AJ, Galjart N, Krangel MS, Tcra gene recombination is supported by a Tcra enhancer- and CTCF-dependent chromatin hub. Proc Natl Acad Sci U S A 109, E3493–3502 (2012). [PubMed: 23169622]

Author Manuscript Author Manuscript Author Manuscript Author Manuscript

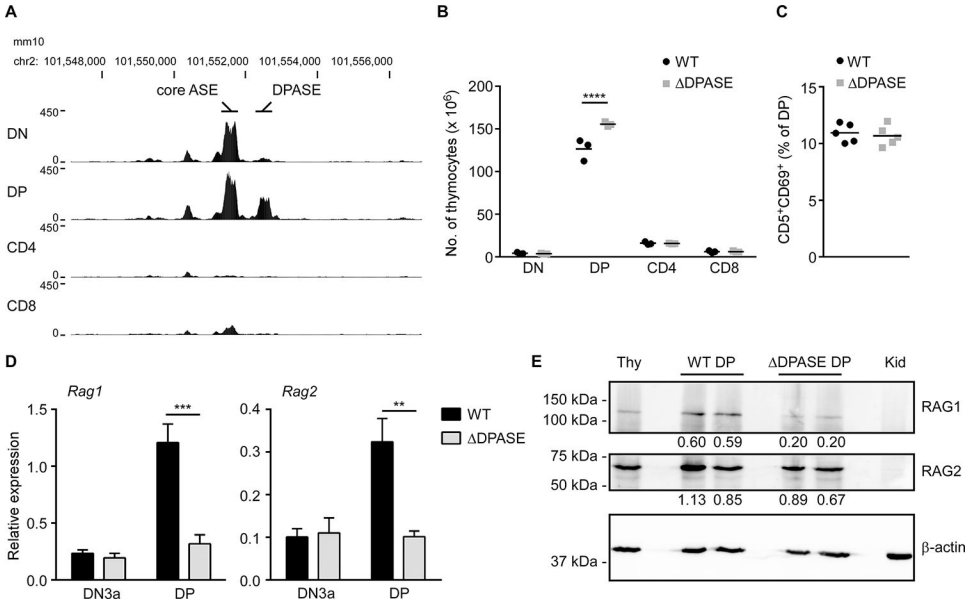

Figure 1.

The DPASE directs RAG gene upregulation in DP thymocytes. **(A)** ASE region ATAC-seq peaks (GSE107076) in DN, DP, CD4SP and CD8SP thymocytes. **(B)** Quantification of thymocyte sub-populations in WT and ΔDPASE mice. Three pairs of WT and ΔDPASE littermate mice were analyzed in three independent experiments. Statistical significance was calculated using two-way ANOVA with Holm-Sidak's correction for multiple comparisons. Each symbol represents an individual mouse; horizontal line represents the mean. (**C**) Quantification of positive selection in ΔDPASE mice. Five pairs of WT and DDPASE littermates were analyzed in five independent experiments. Statistical significance was evaluated by unpaired t-test. **(D)** *Rag1* and *Rag2* transcript levels in DN3a and DP thymocytes measured by qRT-PCR. *Rag1* and *Rag2* transcript levels were normalized to those for *Actb*. The data represent the mean and s.e.m. of three independent experiments analyzing DN3a thymocytes (one littermate pair per experiment) and five independent experiments analyzing DP thymocytes (one littermate pair per experiment). Statistical significance was calculated using two-way ANOVA with Holm-Sidak's correction for multiple comparisons. $^{**}P<0.01$, $^{***}P<0.001$, $^{****}P<0.0001$. **(E)** RAG1 and RAG2 protein abundance measured by immunoblot. Results are presented for sorted DP thymocytes from two pairs of WT and ΔDPASE littermates. Total thymus (Thy) and kidney (Kid) served as positive and negative controls, respectively. Numbers below each lane represent RAG protein expression normalized to that for β-actin.

Author Manuscript Author Manuscript Author Manuscript Author Manuscript

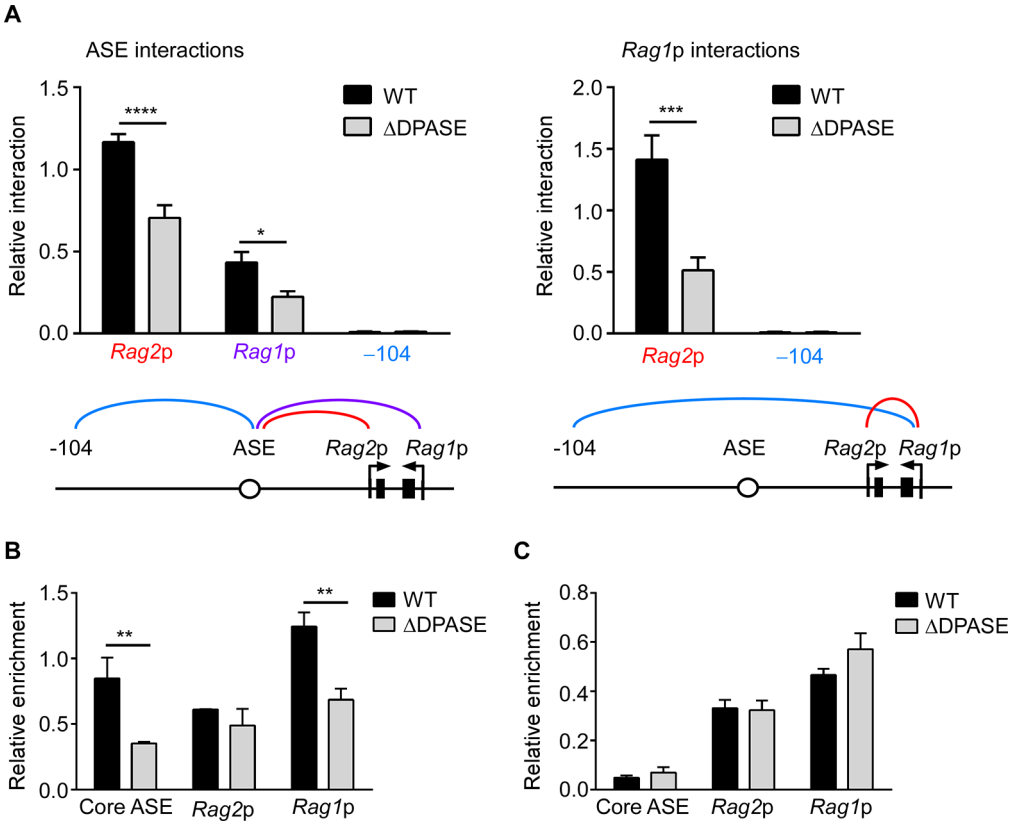

Figure 2.

The DPASE regulates RAG locus conformation and RNA polII loading in DP thymocytes. **(A)** 3C analysis showing interactions from the ASE viewpoint (left) and the *Rag1p* viewpoint (right) in WT and ΔDPASE thymocytes. The −104 fragment served as a negative control. Relative interactions were calculated using BAC standards and were normalized to those of a nearest neighbor restriction fragment. The data represent the mean and s.e.m of four independent experiments, each analyzing a littermate pair. Statistical significance was calculated by two-way ANOVA with Holm-Sidak's correction for multiple comparisons. **(B,C)** ChIP analysis of RNA Pol II (B) and H3K4me3 (C) at the core ASE and RAG promoters in DP thymocytes of WT and ΔDPASE mice. Values were expressed relative to those displayed by the *B2m* promoter. The data represent the mean and s.e.m of three independent experiments, each analyzing a littermate pair. Statistical significance was calculated using two-way ANOVA with Holm-Sidak's correction for multiple comparisons. **P*<0.05, ***P*<0.01, ****P*<0.001, *****P*<0.0001.

Author Manuscript Author Manuscript Author Manuscript Author Manuscript

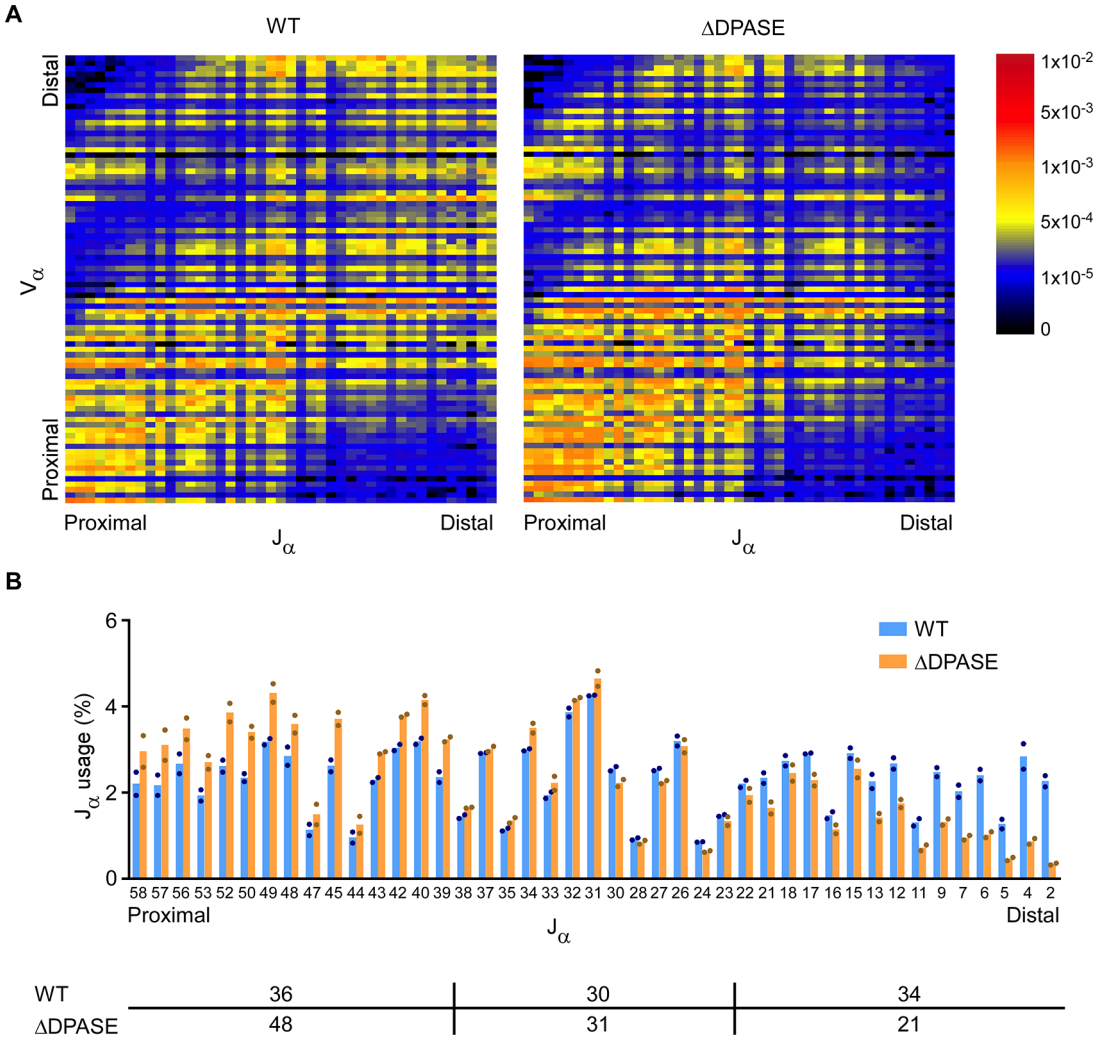

Figure 3.

The DPASE is essential to generate a complete *Tcra* repertoire. **(A)** Heatmaps show frequencies of Vα-Jα rearrangements in $CD4^+CD8^+CD3\varepsilon^{lo}$ thymocytes as measured by 5' RACE and high throughput sequencing. The data represent the results of one of two independent experiments, each analyzing a pair of WT and ΔDPASE littermates. **(B)** Relative usage of Jα segments in WT and ΔDPASE mice. The data represent mean of two independent experiments, each analyzing a pair of WT and ΔDPASE littermates (top). Statistical significance was calculated using two-way ANOVA with Holm-Sidak's correction for multiple comparisons (Table S1). Aggregate usage (%) of the proximal 15, central 13, and distal 15 Jα segments in each genotype (bottom).

Author Manuscript Author Manuscript Author Manuscript Author Manuscript

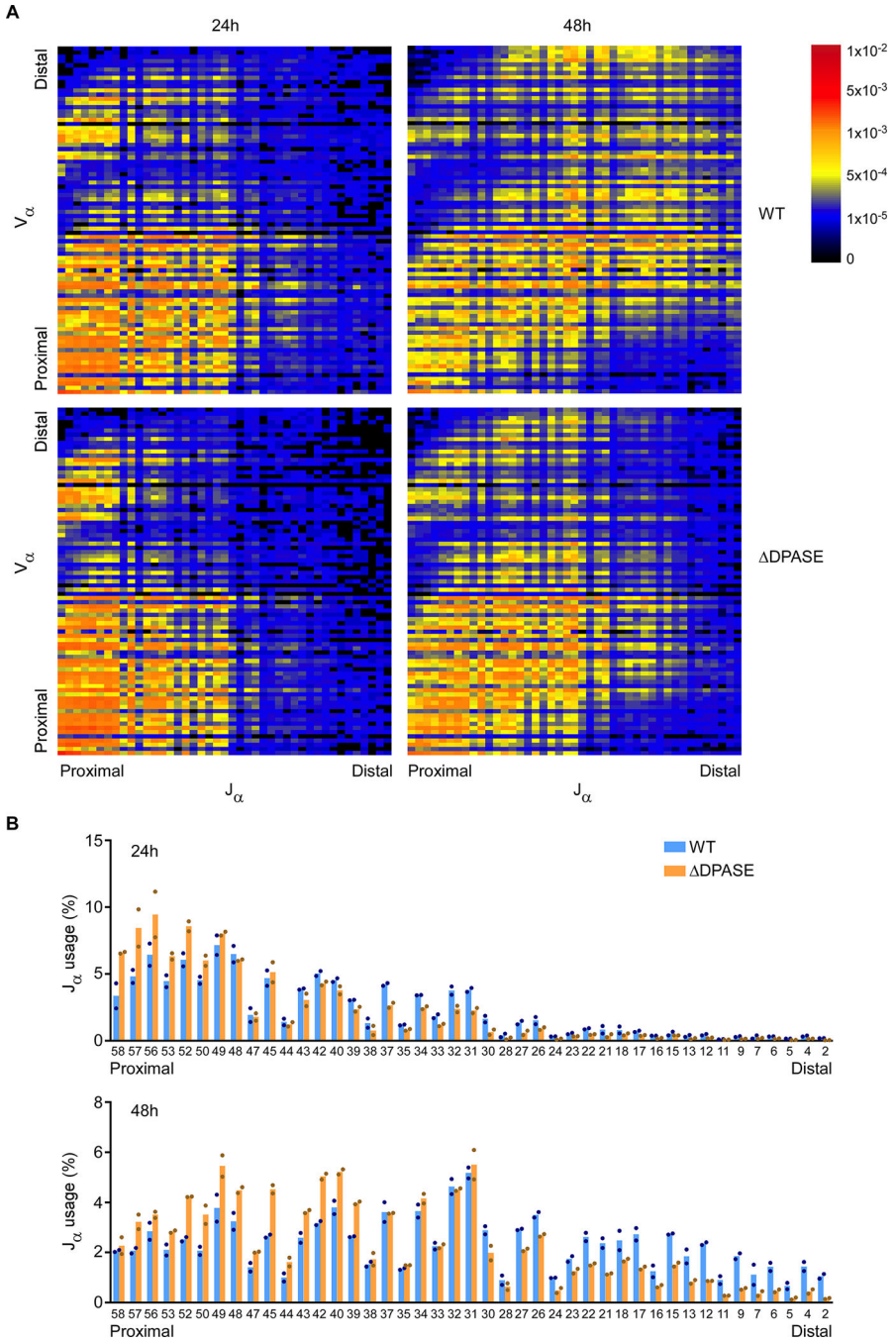

Figure 4.

The DPASE is essential for normal kinetics of secondary *Tcra* recombination. (**A).** Heatmaps showing frequencies of Vα-Jα rearrangements in WT and ΔDPASE ZsG^{+} CD4^{+}CD8^{+}CD3ε^{lo} thymocytes 24h and 48h after tamoxifen injection. The data represent the results of one of two independent experiments per timepoint, each analyzing a pair of WT and ΔDPASE littermates. **(B)** Relative usage of Jα segments in WT and ΔDPASE mice. The data represent mean of two independent experiments per timepoint, each analyzing a

Author Manuscript Author Manuscript Author Manuscript Author Manuscript

pair of WT and ΔDPASE littermates. Statistical significance was calculated using two-way ANOVA with Holm-Sidak's correction for multiple comparisons (Table S1).

Author Manuscript Author Manuscript Author Manuscript Author Manuscript

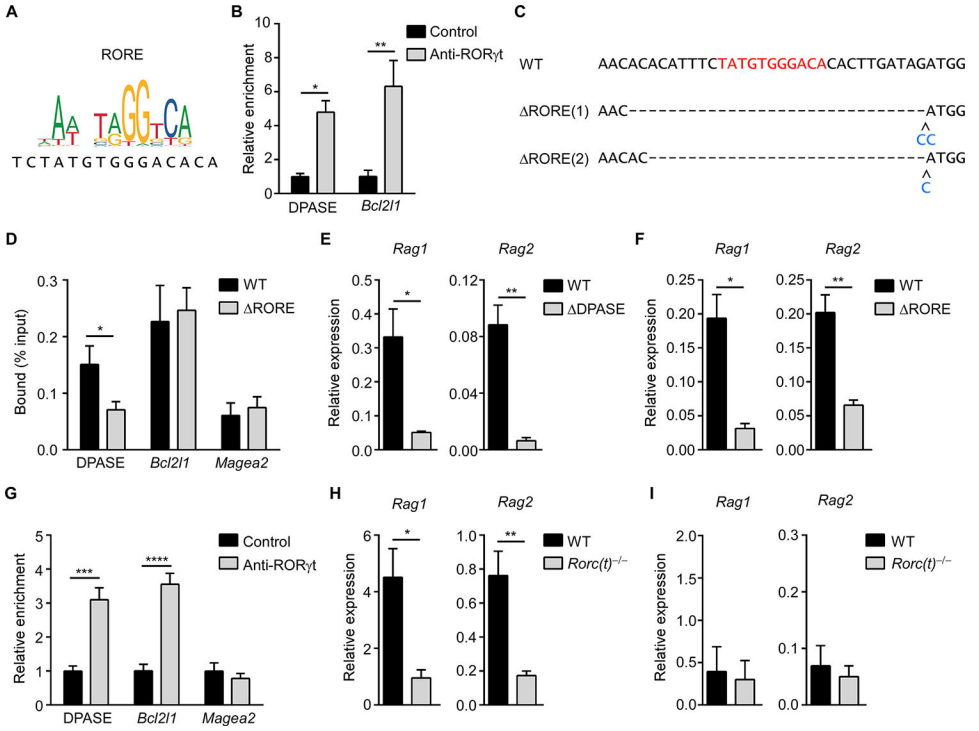

Figure 5.

RORγt regulates RAG expression by binding to the DPASE. **(A)** RORγt sequence logo (Jaspar, 9th release) aligned with DPASE sequence. **(B)** ChIP analysis of RORγt binding to the DPASE and *Bcl2l1* in VL3–3M2 cells. The data are expressed as mean and s.e.m. fold-enrichment over control IgG ChIP in three independent experiments. Statistical significance was evaluated by two-way ANOVA with Holm-Sidak's correction for multiple comparisons. **(C)** CRISPR-Cas9 was used to generate a VL3–3M2 mutant with distinct RORE deletions on the two alleles. The RORE is denoted by red lettering. Inserted nucleotides are denoted by blue lettering. **(D)** ChIP analysis of RORγt binding to the ΔRORE DPASE. The data are expressed as mean and s.e.m. binding (% input) in four independent experiments. Statistical significance was evaluated by two-way ANOVA with Holm-Sidak's correction for multiple comparisons.

(E and F) *Rag1* and *Rag2* expression in WT and ΔDPASE (E), and in WT and ΔRORE (F) VL3–3M2 cells, measured by qRT-PCR. *Rag1* and *Rag2* transcript levels were normalized to those for *Actb*. The data represent the mean and s.e.m. of three independent experiments, each analyzing a pair of littermates. Statistical significance was calculated using unpaired t-test. **(G)** ChIP analysis of RORγt binding in DP thymocytes obtained from anti-CD3ε injected *Rag2*$^{-/-}$ mice. The data represent the mean and s.e.m. fold-enrichment over control in three independent experiments, each analyzing a pair of littermates. Statistical significance was calculated by two-way ANOVA with Holm-Sidak's correction for multiple comparisons. *MageA2* served as a negative control. **(H and I)** *Rag1* and *Rag2* transcript levels in WT and *Rorc(t)*$^{-/-}$ DP (H) and DN (I) thymocytes measured by qRT-PCR with normalization to those for *Actb*. The data represent the mean and s.e.m. of four (H) and five (I) independent experiments, each analyzing a pair of littermates. Statistical significance was calculated by unpaired t-test. *P<0.05, **P<0.01, ***P<0.001, ****P<0.0001.

Author Manuscript Author Manuscript Author Manuscript Author Manuscript

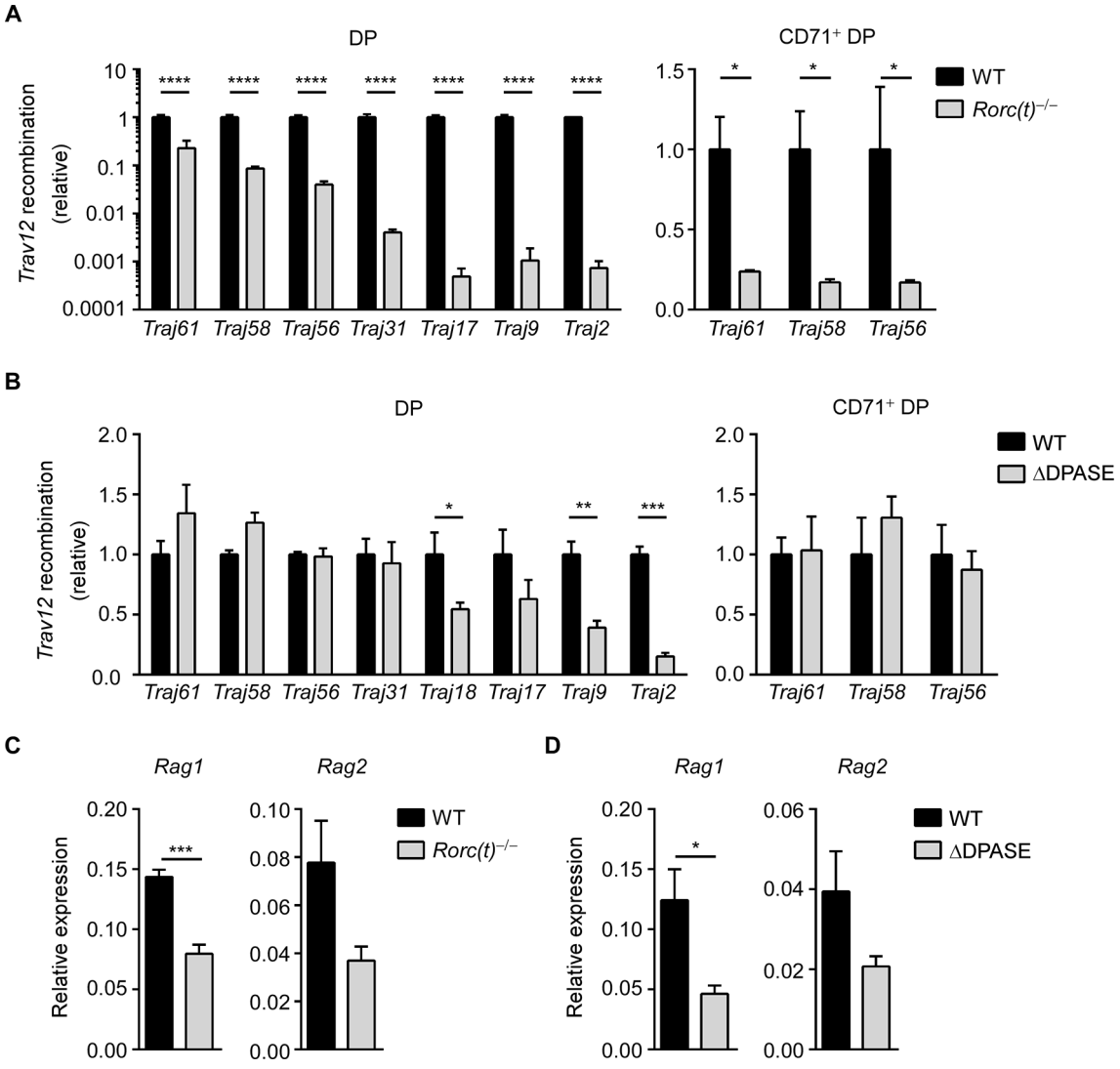

Figure 6.

Both proximal and distal Jα rearrangements are impaired in *Rorc(t)*$^{-/-}$ DP thymocytes. **(A)** *Trav12* family rearrangements to different Jα segments were measured by qPCR of genomic DNA samples of CD3$^{-/low}$ (left) or CD71^{+} (right) DP thymocytes. Rearrangement values for WT and *Rorc(t)*$^{-/-}$ were initially normalized to *Cd14* after which average values for mutant were expressed relative to WT (average value set to 1) for each Jα segment. The data for CD3$^{-/low}$ DP thymocytes represent the mean and s.e.m. of three independent experiments, each analyzing a pair of littermates, with the exception that only two experiments were performed for the *Traj61* datapoint. The data for CD71^{+} DP thymocytes represent the mean and s.e.m. of three independent experiments analyzing four littermate pairs. **(B)** *Trav12* family rearrangements to different Jα segments in CD3$^{-/low}$ (left) or CD71^{+} (right) DP thymocytes of WT and ΔDPASE mice, analyzed as in (A). The data represent the mean and s.e.m. of three independent experiments, each analyzing a pair of littermates. Statistical significance was calculated using two-way ANOVA with Holm-Sidak's correction for multiple comparisons. **(C, D)** *Rag1* and *Rag2* transcript levels in WT and *Rorc(t)*$^{-/-}$

Author Manuscript Author Manuscript Author Manuscript Author Manuscript

$CD71^+$ DP thymocytes (C) or in WT and ΔDPASE $CD71^+$ DP thymocytes, measured by qRT-PCR with normalization to those for *Actb*. The data represent the mean and s.e.m. of four (C) or three (D) independent experiments, each analyzing a pair of littermates. Statistical significance was calculated by unpaired t-test. *P<0.05, **P<0.01, ***P<0.001, ****P<0.0001.

Author Manuscript Author Manuscript Author Manuscript Author Manuscript

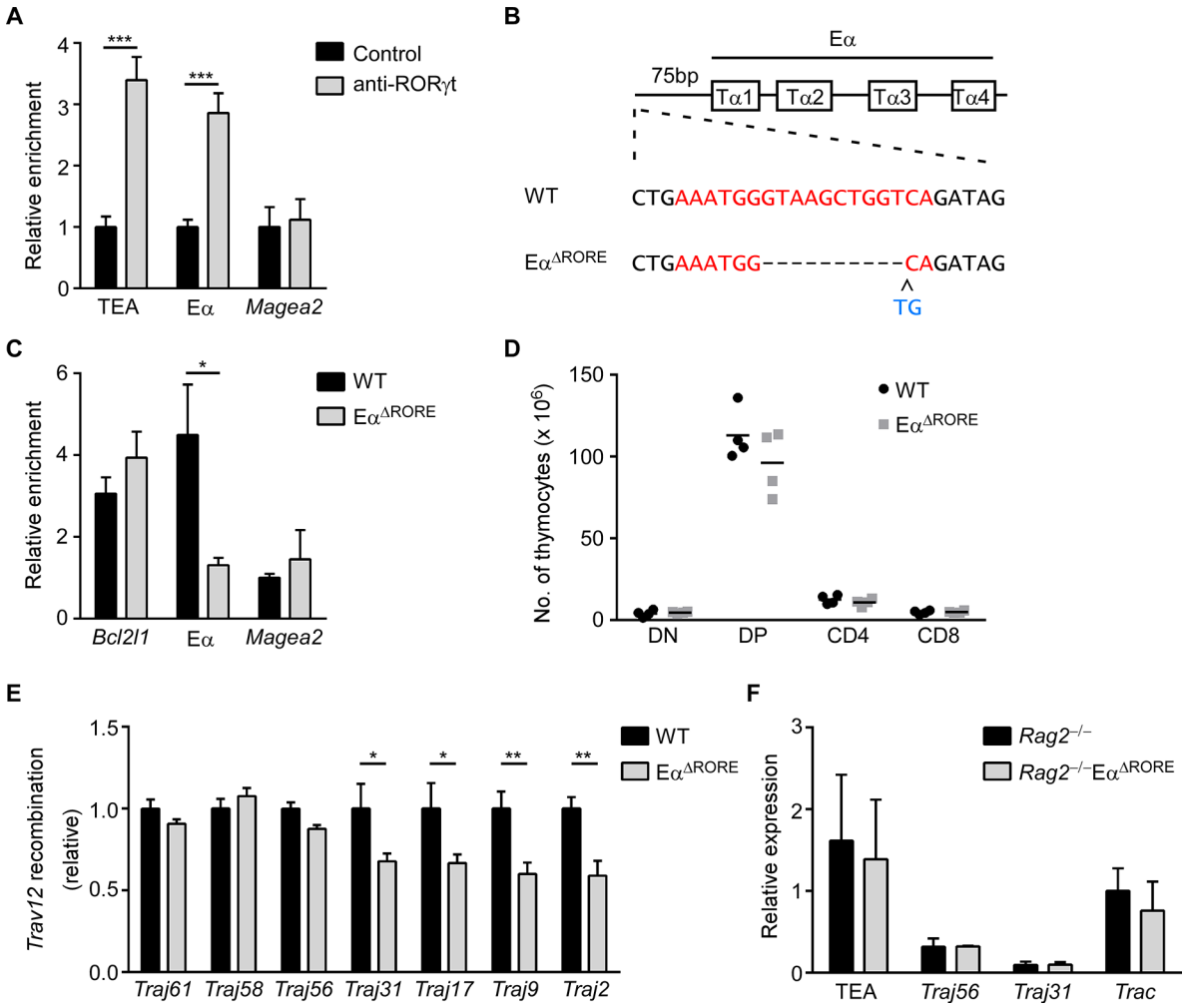

Figure 7.

RORγt regulates the *Tcra* repertoire by direct binding to the *Tcra* locus. **(A)** ChIP analysis of RORγt binding to the *Tcra* locus in DP thymocytes of anti-CD3-injected *Rag2*$^{-/-}$ mice. *Magea2* served as a negative control. The data are expressed as mean and s.e.m. fold-enrichment over control IgG ChIP in four independent experiments. Statistical significance was evaluated by two-way ANOVA with Holm-Sidak's correction for multiple comparisons. **(B)** CRISPR-Cas9 disruption of two overlapping predicted ROREs situated immediately upstream of Eα. The ROREs are denoted by red lettering; a small insertion is denoted by blue lettering. **(C)** Disruption of RORγt binding to Eα measured by ChIP. *Bcl2l1* and *Magea2* served as positive and negative controls, respectively. The data are expressed as mean and s.e.m. fold-enrichment over control IgG ChIP in three independent experiments, each analyzing a littermate pair. Statistical signifiance was evaluated by two-way ANOVA with Holm-Sidak's correction for multiple comparisons. **(D)** Thymocyte populations in WT and Eα$^{\Delta RORE}$ mice. Four pairs of littermates were analyzed in four independent experiments. Statistical significance was calculated using two-way ANOVA with Holm-Sidak's correction for multiple comparisons. **(E)** *Trav12* family rearrangement to different Jα segments measured by qPCR of DP thymocyte genomic DNA samples, with values for

Author Manuscript Author Manuscript Author Manuscript Author Manuscript

WT and Eα$^{\Delta RORE}$ normalized as in Fig 6A. The data represent the mean and s.e.m. of three independent experiments, each analyzing a pair of littermates. Statistical significance was calculated using two-way ANOVA with Holm-Sidak's correction for multiple comparisons. **(F)** *Tcra* germline transcription in DP thymocytes of anti-CD3 injected mice measured by qRT-PCR. Values for *Tcra* germline transcripts were normalized to those for *Hprt* and the average value for *Trac* in WT was then set to 1. The data represent the mean and s.e.m. of three independent experiments, each analyzing a pair of mice. Statistical significance was calculated using two-way ANOVA with Holm-Sidak's correction for multiple comparisons. *P<0.05, **P<0.01, ***P<0.001.